ACS APPLIED BIO MATERIALS

www.acsabm.org Article

# Zwitterionic Polydopamine/Protein G Coating for Antibody Immobilization: Toward Suppression of Nonspecific Binding in Immunoassays

Jihyun Byun, Soojeong Cho, Jeong Moon, Hongki Kim, Hyunju Kang, Juyeon Jung, Eun-Kyung Lim, Jinyoung Jeong, Hyun Gyu Park, Woo Kyung Cho,* and Taejoon Kang*

Cite This: *ACS Appl. Bio Mater.* 2020, 3, 3631−3639 Read Online

ACCESS | Metrics & More | Article Recommendations | Supporting Information

**ABSTRACT:** For the development of immunoassays into sophisticated analyte-sensing methods, it is a priority to suppress nonspecific binding in immunoassays. Herein, we report a one-step surface coating method that can not only optimally immobilize antibodies but also suppress nonspecific binding. Zwitterionic dopamine (*ZW*-DOPA) exhibits distinct antifouling performance, and protein G enables an antibody to have an optimal orientation. A mixture of *ZW*-DOPA and protein G can be simply coated onto various kinds of surfaces, and the antibody can be immobilized onto the *ZW*-DOPA/protein G-coated surfaces. The antifouling property of the zwitterionic group, surface-independent coating property of the catechol and amine groups, and antibody-retaining property of protein G synergistically contribute to surface-independent and oriented immobilization of antibodies without nonspecific binding. The surface characteristics of *ZW*-DOPA/protein G-coated substrates were analyzed by X-ray photoelectron spectroscopy, contact angle goniometry, atomic force microscopy, and ellipsometry. Importantly, the *ZW*-DOPA/protein G-coated substrates showed high resistance to nonspecific protein adhesion. We also verified that antibodies could be immobilized onto *ZW*-DOPA/protein G-coated substrates using fluorescence and biolayer interferometry systems. Finally, *ZW*-DOPA/protein G-coated substrates were employed as immune substrates for influenza virus detection via the naked eye and surface-enhanced Raman scattering, allowing us to efficiently identify the virus. It is anticipated that the developed *ZW*-DOPA/protein G coating method will be useful for the advancement of immunoassays.

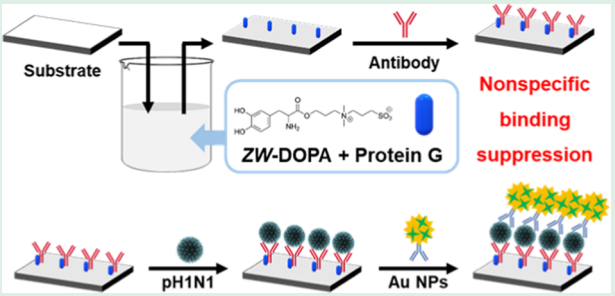


**KEYWORDS:** *zwitterionic dopamine, protein G, antibody immobilization, nonspecific binding, immunoassay, influenza virus, surface-enhanced Raman scattering*



## INTRODUCTION

Immunoassays are one of the most commonly used methods for the analysis of various kinds of biological and chemical species.[1] The simple operation and fine accuracy of immunoassays make them useful in various fields, such as disease diagnosis and prognosis, environmental monitoring, and food safety.[2−4] Recently, immunoassays have been combined with newly developed materials and nanostructures to develop sophisticated analyte detection methods.[5,6] Immunoassays are fundamentally based on the interaction of antibody and antigen; therefore, it is critical to immobilize antibodies onto a surface uniformly with proper orientation.[7] In this regard, numerous strategies have been developed to immobilize antibodies onto several sensor platforms.[8] However, most of the strategies are optimized for individual sensing platforms, lacking wide applicability.[9] This limitation motivated us to develop a surface-independent coating method that can immobilize antibodies onto various sensing platforms. Another critical issue in immunoassays is the prevention of nonspecific binding for accurate assays.[10] Nonspecific binding is occasionally observed in immunoassays, particularly when the sample is included in a complex solution, including serum, extraction buffer, raw environmental solution, etc.[11] To reduce nonspecific binding, blocking reagents, including detergents, proteins, and polymers, have generally been employed.[12] These reagents block the unoccupied areas of sensor surfaces, suppressing nonspecific binding.[11,12] If a one-step coating procedure enables us to optimally immobilize antibodies onto any surface and to suppress nonspecific binding, the method can be applied to various immunosensing platforms, leading to future advances in immunoassays.

Received: March 7, 2020
Accepted: April 20, 2020
Published: April 20, 2020

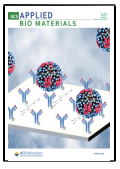





https://dx.doi.org/10.1021/acsabm.0c00264
*ACS Appl. Bio Mater.* 2020, 3, 3631−3639

Polydopamine (PDA) coating is regarded as a simple functionalization method for virtually any material surface.[13,14] Previous literature demonstrated that the use of PDA coating was effective for metal−organic frameworks, synthetic polyolefin membranes, composite materials, nanostructured surfaces showing superhydrophobicity or superoleophobicity, etc.[15,16] Consequently, the applications of PDA coatings are growing exponentially and include antimicrobial surfaces, cell culture/patterning, tissue engineering, microfluidics, biosensing, photothermal therapy, drug delivery systems, immobilization of photocatalysts, and others.[17,18] Previously, our group developed a simple surface modification method that can optimally immobilize antibodies onto various surfaces using PDA and protein G. This method not only reduced the need for inconvenient surface modification procedures for antibodies but also expanded the types of materials used for immunosensors.[19] However, the PDA coating itself could not suppress nonspecific binding;[20] thus, bovine serum albumin (BSA) was used as a blocking reagent.[19] Herein, we further advanced the antibody immobilization method by employing zwitterionic dopamine (*ZW*-DOPA). Since zwitterionic (ZW) polymers have unique anti-polyelectrolyte behavior, they exhibit distinct antifouling performance.[21] In addition, *ZW*-DOPA has surface-independent coating capability and one-step coating ability with other molecules.[23] On the basis of these properties, we speculated that simple, surface-independent, and oriented immobilization of antibodies with the suppression of nonspecific binding is possible by combining *ZW*-DOPA and protein G. The antifouling property of the ZW group, the surface-independent coating property of catechol and amine groups, and the antibody-retaining property of protein G can synergistically contribute to the surface-independent and oriented immobilization of antibodies without nonspecific binding.[21,24,25]

In this report, we show that one-step *ZW*-DOPA/protein G coating enables substrate-independent immobilization of antibodies and nonspecific binding suppression. The surface of *ZW*-DOPA/protein G-coated substrates was characterized by X-ray photoelectron spectroscopy (XPS), contact angle goniometry, atomic force microscopy (AFM), and ellipsometry. Moreover, we verified that the *ZW*-DOPA/protein G coating could markedly reduce nonspecific protein adsorption. The fluorescence and biolayer interferometry analyses clearly proved antibody immobilization onto the *ZW*-DOPA/protein G-coated substrates. Furthermore, we applied *ZW*-DOPA/protein G-coated substrates for immunoassays of influenza A/CA/07/2009 (pH1N1). After the immunoreactions, the pH1N1 influenza virus could be identified by the naked eye and by surface-enhanced Raman scattering (SERS) observation. Importantly, nonspecific binding was suppressed on the *ZW*-DOPA/protein G-coated substrates, allowing us to efficiently detect the influenza virus. The novelty of the current work is summarized as follows: (1) It is proved that antibodies can be routinely immobilized onto the *ZW*-DOPA/protein G-coated substrate. (2) The *ZW*-DOPA/protein G coating effectively prevents nonspecific binding without further blocking steps. (3) The *ZW*-DOPA/protein G-coated substrates can be excellent immune substrates for the detection of the influenza virus. On the basis of these results, we expect that the *ZW*-DOPA/protein G coating will be used for several kinds of immunosensing approaches and will contribute to advances in immunoassays.

## RESULTS AND DISCUSSION

Figure 1 shows a schematic procedure for *ZW*-DOPA/protein G coating and antibody immobilization onto a substrate. *ZW*-

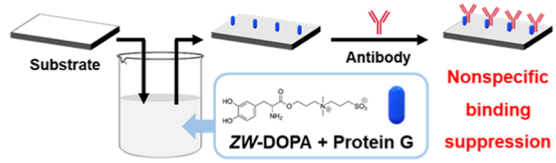


**Figure 1.** Schematic procedure of *ZW*-DOPA/protein G coating and antibody immobilization onto a bare substrate.

DOPA was synthesized through coupling of (3,4-dihydroxyphenyl)-L-alanine (DOPA) with 3-(dimethylamino)-1-propanol followed by zwitterionization with 1,3-propane-sultone, producing a sulfobetaine compound.[26] The synthesized *ZW*-DOPA was mixed with ammonium persulfate, and then the mixture was added to a protein G solution. For *ZW*-DOPA/protein G coating, a bare substrate was incubated in the *ZW*-DOPA/protein G solution and washed. Next, the *ZW*-DOPA/protein G-coated substrate was incubated with an antibody and washed. Using these simple procedures, we could obtain a well-oriented antibody on a substrate that can act as an immune substrate.

It is well known that dopamine and DOPA derivatives, including *ZW*-DOPA, can coat various substrates under oxidation conditions.[18,21,22] Moreover, the molecules codissolved with *ZW*-DOPA can also be coated onto the substrates during incubation.[14,22,27,28] Therefore, *ZW*-DOPA/protein G-coated substrates can be obtained after the simple incubation of bare substrates in the *ZW*-DOPA/protein G solution, as shown in Figure 1. Protein G is an antibody-binding protein that can target the Fc region of an antibody.[25,29] Hence, the antibody can be routinely immobilized onto the *ZW*-DOPA/protein G-coated substrate. In the previous literature, it has been verified that the protein G-bound antibody is well exposed to antigen, thus improving the sensitivity in immunoassays.[25,29] More importantly, *ZW*-DOPA can exhibit a distinct antifouling performance.[21] Considering that the prevention of nonspecific binding is a critical issue in immunoassays,[10] the antifouling property of *ZW*-DOPA can be beneficial for accurate immunoassays. Taken together, the results show that the *ZW*-DOPA/protein G-coated substrates enable us to immobilize antibodies with proper orientation and reduce nonspecific binding without additional blocking steps.

Figure 2 shows the XPS analysis results of bare glass, *ZW*-DOPA-coated glass, and *ZW*-DOPA/protein G-coated glass substrates. Compared with the results for bare glass, after the *ZW*-DOPA coating, N 1s and S 2p peaks newly appeared and the atomic composition of C 1s increased, with decrease in those of Si 2p and O 1s. This result indicates the successful coating of *ZW*-DOPA on a glass substrate. After the *ZW*-DOPA/protein G coating, the atomic compositions of C 1s and N 1s greatly increased and those of O 1s, Si 2p, and S 2p decreased. Considering that the main chemical elements of protein G are C and N, this XPS result supports the simultaneous coating of *ZW*-DOPA and protein G on the glass substrate. The formation of *ZW*-DOPA layers on glass substrates was further investigated with contact angle goniometry (Figure 3a). The static water contact angle on the bare glass substrate was 55.0 ± 1.7°, and the angle


https://dx.doi.org/10.1021/acsabm.0c00264
ACS Appl. Bio Mater. 2020, 3, 3631−3639

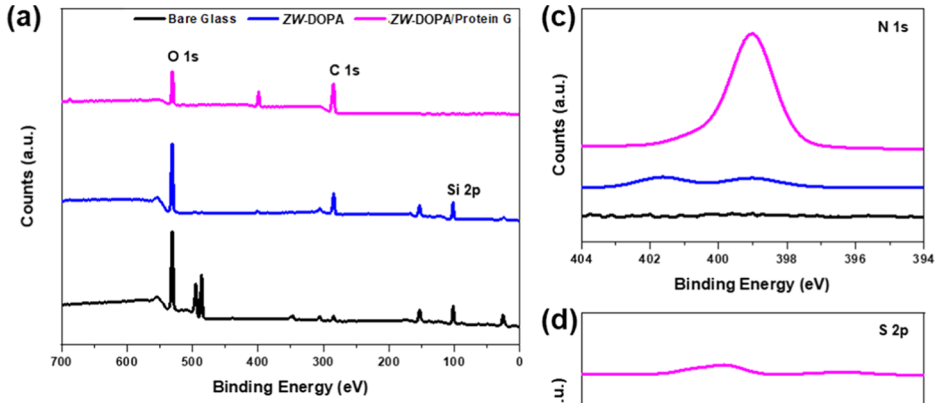


(b)

Atomic composition (%)

| | C 1s | N 1s | O 1s | Si 2p | S 2p |
|---|---|---|---|---|---|
| Bare Glass | 9.53 | 0.41 | 66.19 | 23.81 | 0.06 |
| *ZW*-DOPA | 32.80 | 2.71 | 44.91 | 17.95 | 1.63 |
| *ZW*-DOPA/ Protein G | 64.12 | 14.52 | 20.19 | 0.69 | 0.49 |

**Figure 2.** (a) XPS analysis results of bare (black), *ZW*-DOPA-coated (blue), and *ZW*-DOPA/protein G-coated (magenta) glass substrates. (b) Surface atomic composition of bare, *ZW*-DOPA-coated, and *ZW*-DOPA/protein G-coated glass substrates. (c, d) High-resolution XPS spectra of bare (black), *ZW*-DOPA-coated (blue), and *ZW*-DOPA/protein G-coated (magenta) glass substrates.

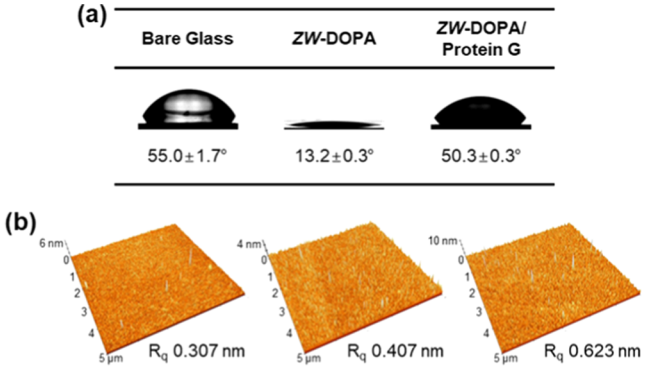


**Figure 3.** (a) Static water contact angle on bare, *ZW*-DOPA-coated, and *ZW*-DOPA/protein G-coated glass substrates. (b) AFM images of bare, *ZW*-DOPA-coated, and *ZW*-DOPA/protein G-coated glass substrates.

decreased to 13.2 ± 0.3° after *ZW*-DOPA coating. This hydrophilicity of the *ZW*-DOPA coating is consistent with the literature.[26] Zwitterions have ultralow fouling properties because of the strong hydration layer formed, which makes the replacement of surface-bound water molecules with foulants enthalpically unfavorable.[30,31] After the *ZW*-DOPA/protein G coating, the static water contact angle was 50.3 ± 0.3°, showing that the combined coating was more hydrophobic than only the *ZW*-DOPA coating. Since protein G has the residues that form the hydrophobic surface cluster,[32] this wettability indicates that *ZW*-DOPA and protein G were coated together on the substrate. The AFM analysis also indicated the successful coating of *ZW*-DOPA and *ZW*-DOPA/protein G on the substrates. The root-mean-square roughness ($R_q$) slightly increased after the *ZW*-DOPA and *ZW*-DOPA/protein G coatings compared to that of the bare glass substrate (Figure 3b). The thickness of the *ZW*-DOPA/protein G film was measured as 4.11 ± 0.16 nm by ellipsometry.

To evaluate the antifouling property of *ZW*-DOPA, we examined the protein adhesions on various substrates (bare, PDA-coated, PDA/protein G-coated, *ZW*-DOPA-coated, and *ZW*-DOPA/protein G-coated glass substrates). Each substrate was soaked in a green fluorescent protein (GFP) solution, gently washed, and monitored under a fluorescence microscope. As shown in Figure 4a, a large amount of GFP was observed on the bare glass substrate. After applying the PDA and PDA/protein G coatings, GFP was still observable on the substrates (Figure 4b,c). Notably, the *ZW*-DOPA-coated substrate showed remarkably reduced adhesion of GFP (Figure 4d). A sparse distribution of GFP was observed after *ZW*-DOPA coating. The adhesion of GFP was also suppressed after coating with the *ZW*-DOPA/protein G mixture (Figure 4e). This observation suggests that the *ZW*-DOPA/protein G-coated substrate may prevent the nonspecific binding of proteins in immunoassays. Figure 4f presents the plot of green fluorescence intensity on a variety of substrates, clearly showing that the fluorescence intensity was reduced after coating with *ZW*-DOPA or *ZW*-DOPA/protein G. The antifouling property of *ZW*-DOPA was further proved by the fluorescence images of *Escherichia coli* attached to the bare, *ZW*-DOPA-coated, and *ZW*-DOPA/protein G-coated glass substrates (Figure S1). The substrates were treated with $10^4$ CFU/mL *E. coli* cultured in Luria-Bertani (LB) broth at 37 °C. After incubation at 37 °C for 18 h, the substrates were washed three times, immersed in a dye solution (3 $\mu$M SYTO9 and 3 $\mu$M propidium iodide) at room temperature for 20 min, and observed by fluorescence microscopy. The *ZW*-DOPA-coated and *ZW*-DOPA/protein G-coated glass substrates showed no fluorescence signals.

Next, we investigated the immobilization of an antibody onto the *ZW*-DOPA/protein G-coated substrate. For the investigation, an Alexa647-conjugated antibody was employed. Figure 5a displays fluorescence images of various substrates (bare, PDA-coated, PDA/protein G-coated, *ZW*-DOPA-coated, and *ZW*-DOPA/protein G-coated glass substrates) after fluorescent antibody immobilization. When protein G was


https://dx.doi.org/10.1021/acsabm.0c00264
ACS Appl. Bio Mater. 2020, 3, 3631−3639

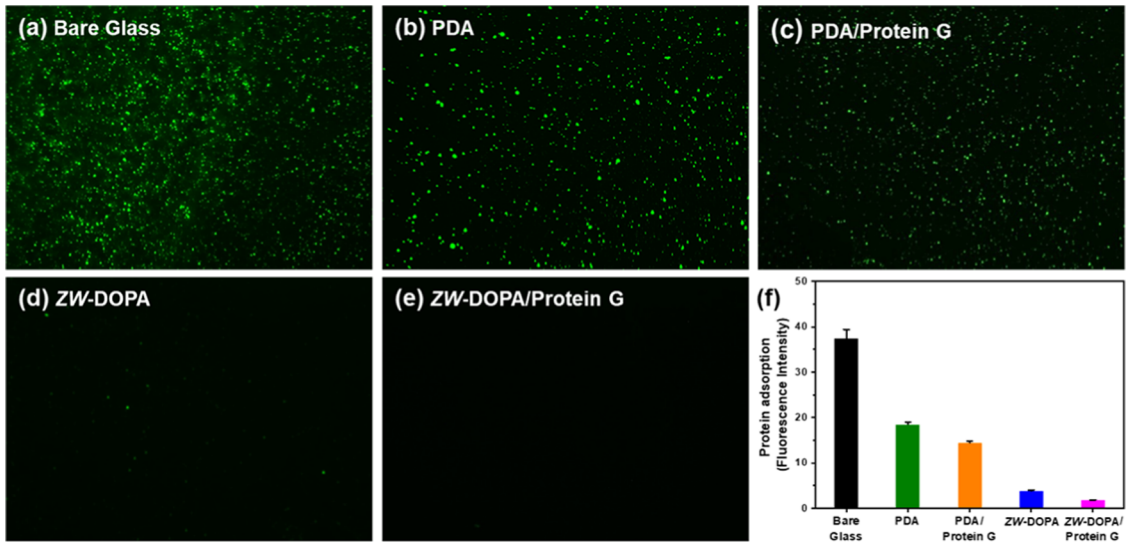


**Figure 4.** Fluorescence images of GFPs attached to (a) bare, (b) PDA-coated, (c) PDA/protein G-coated, (d) *ZW*-DOPA-coated, and (e) *ZW*-DOPA/protein G-coated glass substrates. (f) Corresponding plot of fluorescence intensity on bare (black), PDA-coated (green), PDA/protein G-coated (orange), *ZW*-DOPA-coated (blue), and *ZW*-DOPA/protein G-coated (magenta) glass substrates.

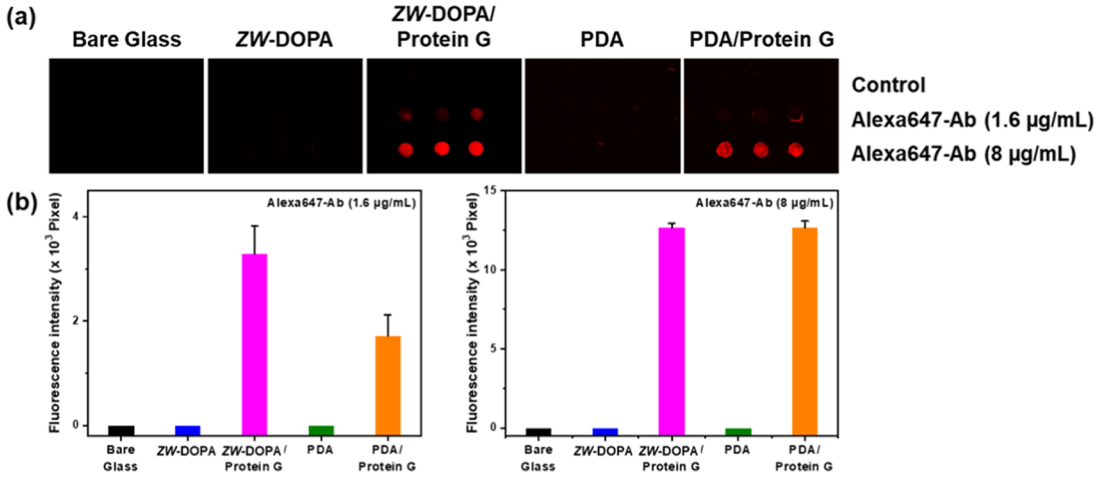


**Figure 5.** (a) Fluorescence images of bare, *ZW*-DOPA-coated, *ZW*-DOPA/protein G-coated, PDA-coated, and PDA/protein G-coated glass substrates after Alexa647-conjugated antibody immobilization. (b) Corresponding plots of fluorescence intensity on bare (black), *ZW*-DOPA-coated (blue), *ZW*-DOPA/protein G-coated (magenta), PDA-coated (green), and PDA/protein G-coated (orange) glass substrates after Alexa647-conjugated antibody immobilization.

present on the substrate, bright fluorescent spots were obtained. This result indicated that the antibody was efficiently immobilized in the presence of protein G. The plot of fluorescence intensity on the substrates further proved that the antibody was immobilized on the *ZW*-DOPA/protein G- and PDA/protein G-coated substrates (Figure 5b). When 8 $\mu$g of Alex647-Ab was used, strong fluorescence signals were observed from both *ZW*-DOPA/protein G- and PDA/protein G-coated substrates. When 1.6 $\mu$g of Alex647-Ab was employed, stronger signals were obtained from the *ZW*-DOPA/protein G-coated substrate than from the PDA/protein G-coated substrate. This result may be attributed to the antifouling property of *ZW*-DOPA. For the optimization of the *ZW*-DOPA/protein G coating and antibody immobilization, we varied the concentration of protein G (0.5, 2.5, 5, 10, 15, 20, and 25 mg/mL) in the *ZW*-DOPA/protein G mixture. As the concentration of protein G increased from 0.5 to 10 mg/mL, more fluorescent antibodies could be immobilized on the *ZW*-DOPA/protein G-coated substrate (Figure S2). At more than 10 mg/mL protein G, the fluorescence intensity was saturated. Therefore, the optimal *ZW*-DOPA and protein G mixture was estimated as a 1:1 volume mixture of *ZW*-DOPA (2 mg/mL) and protein G (20 mg/mL).

The antibody immobilization on the *ZW*-DOPA/protein G-coated substrate was further verified by the biolayer interferometry system. The tip surfaces of the sensor systems were coated separately with PDA, PDA/protein G, *ZW*-DOPA, and *ZW*-DOPA/protein G. After coating, the antibody was loaded on the tip surface and washed with buffer. Figure 6 shows the sensorgram measured by the biolayer interferometry system during the antibody loading and washing steps. The binding curves increased significantly on the PDA/protein G- and *ZW*-DOPA/protein G-coated substrates and remained high even after washing (orange and magenta curves). This observation clearly indicates that the antibodies were well immobilized on the protein G-coated substrates. Meanwhile,


https://dx.doi.org/10.1021/acsabm.0c00264
ACS Appl. Bio Mater. 2020, 3, 3631−3639

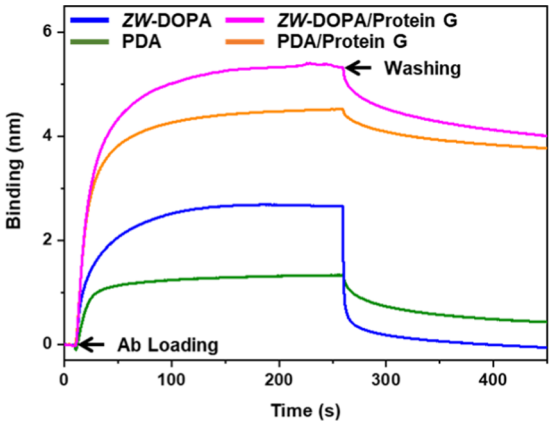


**Figure 6.** Sensorgrams measured by biolayer interferometry systems during antibody loading and washing. On the tip surfaces of bare sensor systems, PDA (green), PDA/protein G (orange), *ZW*-DOPA (blue), and *ZW*-DOPA/protein G (magenta) were coated. After coating, the antibody was loaded on the tip surfaces and washed.

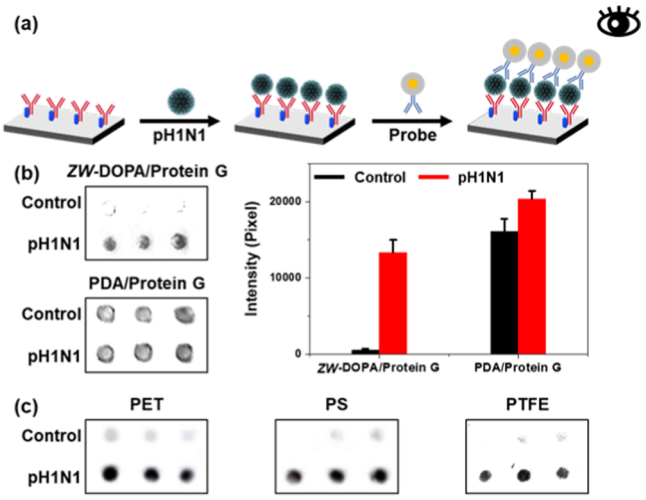


**Figure 7.** (a) Schematic procedures for pH1N1 detection with the naked eye using the *ZW*-DOPA/protein G-coated substrate. (b) Grayscale images of *ZW*-DOPA/protein G-coated (upper) and PDA/protein G-coated (lower) substrates after pH1N1 detection with the naked eye; the corresponding plot of 8-bit grayscale values on *ZW*-DOPA/protein G-coated and PDA/protein G-coated substrates after pH1N1 detection (right). (c) Grayscale images of *ZW*-DOPA/protein G-coated poly(ethylene terephthalate) (PET) (left), polystyrene (PS) (middle), and poly(tetrafluoroethylene) (PTFE) (right) substrates after pH1N1 detection with the naked eye.

the binding curves slightly increased on the PDA- and *ZW*-DOPA-coated substrates during the antibody loading step but decreased after washing (green and blue curves). This result suggests that the antibodies were not immobilized on substrates without protein G coating. Additionally, we found that a small amount of antibody remained on the PDA-coated substrate after washing (green curve). This residual may contribute to the nonspecific adsorption of the antibody. On the *ZW*-DOPA-coated substrate, the binding curve decreased to the baseline after washing (blue curve). This result shows that the antifouling property of *ZW*-DOPA completely prevents the nonspecific adsorption of the antibody. We concluded that the *ZW*-DOPA/protein G-coated substrate could be used for well-oriented antibody immobilization and nonspecific binding suppression.

For detection of the influenza A/CA/07/2009 (pH1N1) virus, the *ZW*-DOPA/protein G-coated substrate was employed. Since influenza viruses cause acute respiratory diseases and thus induce massive economic losses to the society each year,[33] many influenza virus sensing methods have been developed.[34] For instance, immune reaction-based diagnosis methods, such as rapid influenza diagnostic tests and enzyme-linked immunosorbent assays, have been widely used.[35,36] Moreover, advanced sensing approaches have been developed using nanobiotechnology, improving the sensitivity and accuracy of influenza virus diagnosis.[37,38] Accordingly, it is important to apply this novel surface modification technology, which can immobilize an antibody optimally onto any surface and suppress nonspecific binding, to immunoassays of the influenza virus. To investigate whether the *ZW*-DOPA/protein G-coated substrate can act as an immune substrate for pH1N1 detection, we first tried to identify pH1N1 with the naked eye, as displayed in Figure 7a. The bare glass substrate was coated with the *ZW*-DOPA/protein G mixture, and the polyclonal anti-influenza A H1N1 antibody was immobilized on the *ZW*-DOPA/protein G-coated substrate. This antibody-immobilized substrate was reacted with the pH1N1 virus and washed. Next, the pH1N1-captured substrate was immersed in the probe Au nanoparticle (NP) solution, which was prepared by mixing monoclonal anti-influenza A H1N1 antibody, gold-binding peptide (GBP)-protein G, and Au NPs. Finally, the probe Au NPs were enhanced for naked-eye detection of the pH1N1 virus. The upper panel of Figure 7b depicts the grayscale image after the naked-eye detection of the pH1N1 influenza virus using the *ZW*-DOPA/protein G-coated substrate. When the control sample was tested, very faint spots were shown. When the pH1N1 sample was tested, dark spots were clearly observed. This result confirms that the *ZW*-DOPA/protein G-coated substrate can be used for the detection of the influenza virus. For comparison, we also tried to detect pH1N1 using the PDA/protein G-coated substrate. As shown in the lower panel of Figure 7b, it was difficult to identify the pH1N1 virus on the PDA/protein G-coated substrate because dark spots were observed in both the control and pH1N1 samples. Previously, we reported that the PDA/protein G-coated substrate could be applied to the detection of influenza virus. In our previous experiments, the PDA/protein G-coated substrate was blocked with BSA to suppress nonspecific binding.[19] In this experiment, the BSA blocking step was intentionally omitted and thus the control signals were highly enhanced. The spots in the control sample were attributed to the nonspecific adsorption of probe NPs and consequent enhancements. It is noteworthy that the *ZW*-DOPA/protein G-coated substrate can identify pH1N1 without the BSA blocking process. Since the *ZW*-DOPA/protein G-coated substrate has antifouling properties, the substrate can reduce the nonspecific binding of NPs and allow us to detect pH1N1 successfully. The right plot in Figure 7b presents the plot of 8-bit grayscale values as a function of the substrate, further supporting that the *ZW*-DOPA/protein G-coated substrate exhibits better sensing performance in the pH1N1 immunoassay than the PDA/protein G-coated substrate.

*ZW*-DOPA has a universal coating property similar to that of PDA.[39] Therefore, we coated a *ZW*-DOPA/protein G mixture onto various substrates (poly(ethylene terephthalate) (PET), polystyrene (PS), and poly(tetrafluoroethylene) (PTFE)). Figures 7c and S3 show the naked-eye sensing results of the


https://dx.doi.org/10.1021/acsabm.0c00264
ACS Appl. Bio Mater. 2020, 3, 3631−3639

influenza virus on the *ZW*-DOPA/protein G-coated PET, PS, and PTFE substrates. Dark spots were distinctly observable only in the presence of pH1N1. After *ZW*-DOPA/protein G coating, pH1N1 could be identified regardless of the substrate. This result suggests that the *ZW*-DOPA/protein G mixture can be coated onto various kinds of surfaces and that the antibody can be immobilized uniformly on the surfaces. The universal coating property of *ZW*-DOPA can broaden the application of the current method to numerous immunoreaction-based approaches.

For precise detection of pH1N1, the *ZW*-DOPA/protein G-coated substrate was adopted as an immune substrate in a SERS-based immunoassay. SERS is a fascinating phenomenon in which Raman signals of molecules are significantly enhanced at hot spots.[40] Because of the single-molecule-level sensitivity, fingerprint spectrum, and insensitivity to quenching, SERS has been attractive for disease diagnosis and prognosis, food and environmental monitoring, etc.[40,41] Figure 8a shows a schematic illustration of pH1N1 detection through a SERS-based immunoassay. The *ZW*-DOPA/protein G-coated substrate was prepared and the polyclonal pH1N1 antibody was immobilized as described above. This immune substrate was incubated with pH1N1 and washed. Next, the urchin-like Au NP reporter was reacted with the pH1N1-captured substrate and washed. Finally, SERS signals were obtained. Before pH1N1 detection, the surface of the urchin Au NPs was simultaneously modified by monoclonal pH1N1 antibody and malachite green isothiocyanate (MGITC), a Raman reporter that has a strong absorbance peak near 630 nm.[42,43] Figure S4 shows the absorbance spectrum of the urchin Au NPs, and the inset presents a transmission electron microscopy (TEM) image of the urchin Au NPs. These urchin Au NPs can provide high SERS enhancement because strong electromagnetic fields are generated in the NPs.[44] Figure 8b shows the SERS spectra of MGITC obtained after the SERS-based immunoassays for various concentrations of the pH1N1 virus. From the control sample, only background signals were obtained. As the concentration of the influenza virus increased from 10 to $10^7$ PFU/mL, the SERS signals of MGITC gradually increased. This result shows that precise detection of the pH1N1 virus is feasible through the SERS-based immunoassay on the *ZW*-DOPA/protein G-coated substrate. Figure S5 presents the plot of the 1615 $cm^{-1}$ band intensity as a function of the virus concentration, suggesting the quantitative sensing of pH1N1, with a detection limit of $10^2$ PFU/mL. To examine the selectivity of the SERS-based immunoassay, we tested four types of viruses (pH1N1, H3N2, H5N2, and influenza B virus). The concentration of each virus was $10^6$ PFU/mL. As shown in Figure 8c, the 1615 $cm^{-1}$ band intensity was strongly enhanced only in the presence of pH1N1, whereas weak intensities were observed in the presence of H3N2, H5N2, and influenza B virus. This outcome verified the specificity of the current SERS-based immunoassay for pH1N1. The *ZW*-DOPA/protein G coating method offers the properties of universal coating, well-oriented antibody immobilization, and antifouling. Therefore, we expect that the *ZW*-DOPA/protein G coating method can serve as an excellent antibody interfacing technique for immunoassays.

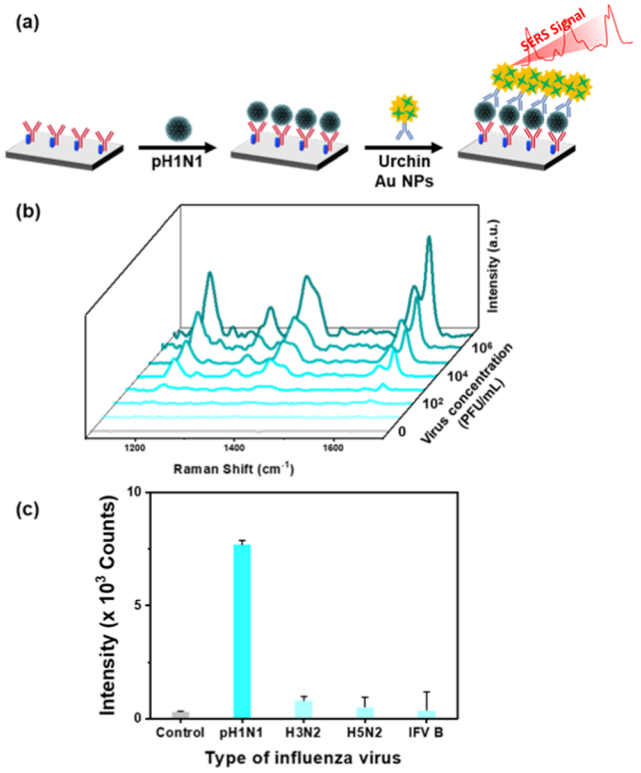


**Figure 8.** (a) Schematic procedures for SERS-based pH1N1 detection using the *ZW*-DOPA/protein G-coated substrate. (b) SERS spectra of MGITC measured from *ZW*-DOPA/protein G-coated substrates after the detection of various concentrations of pH1N1 (0–$10^7$ PFU/mL). (c) Plot of the 1615 $cm^{-1}$ band intensity as a function of the influenza virus type. The concentration of each virus was $10^6$ PFU/mL.

## CONCLUSIONS

We report a one-step *ZW*-DOPA/protein G coating method on a variety of surfaces, enabling oriented immobilization of antibodies and suppression of nonspecific binding. The surface characteristics of the *ZW*-DOPA/protein G-coated substrates were examined by XPS, contact angle goniometry, AFM, and ellipsometry. The *ZW*-DOPA/protein G-coated substrate showed excellent antifouling properties, preventing the nonspecific adsorption of protein. Antibody immobilization on the *ZW*-DOPA/protein G-coated substrate was confirmed by a fluorescence and biolayer interferometry system. Furthermore, the *ZW*-DOPA/protein G-coated substrates were employed as immune substrates for influenza virus detection, allowing us to identify pH1N1 by the naked eye and with SERS measurements. Considering the ease of use and universal coating capability, the current surface modification method will be applicable to various kinds of substrates and provide an efficient and convenient way to develop immune sensors.

## EXPERIMENTAL SECTION

**Materials.** Dopamine hydrochloride, ammonium persulfate (98%), Au NPs, Ag enhancer solutions A and B, and Au(III) chloride trihydrate, Tris–HCl, phosphate-buffered saline (PBS), Tween 20, nonfat milk, and 4-(2-hydroxyethyl)-1-piperazineethanesulfonic acid (HEPES) were purchased from Sigma-Aldrich. Protein G, GFP, SYTO9, and propidium iodide were purchased from Thermo Fisher Scientific. GBP-protein G was purchased from Bioprogen (Korea). Alexa Fluor 647-Fluor Nanogold rabbit anti-goat lgG (H + L) was purchased from Nanoprobes. Pandemic H1N1 virus (A/California/07/2009) (pH1N1), influenza A/Brisbane/10/2007 (H3N2), influenza A/aquatic bird/Korea/2351/2008 (H5N2), influenza B/Victoria/Brisbane/60/208 (IFV B), and *E. coli* were provided as described previously.[19,45,46] The monoclonal anti-influenza A H1N1


https://dx.doi.org/10.1021/acsabm.0c00264
ACS Appl. Bio Mater. 2020, 3, 3631–3639

antibody was purchased from Abcam. The polyclonal anti-influenza A H1N1 antibody was purchased from Sino Biological. MGITC was purchased from Setareh Biotech. Microscopy slides were purchased from Marienfeld (Germany). PS, PTFE, and PET substrates were purchased from a local market in Korea.

**Surface Modification.** For *ZW*-DOPA coating on the substrates, as-synthesized *ZW*-DOPA was dissolved in Tris−HCl buffer (10 mM, pH 8.5) at a concentration of 2 mg/mL. The *ZW*-DOPA solution was then mixed with ammonium persulfate at a molar ratio of 2:1 in pure water. Next, a substrate was incubated in the mixture of *ZW*-DOPA and ammonium persulfate at room temperature for 2 h. Finally, the substrate was sequentially washed with PBS buffer, including 0.1% Tween 20 and pure water. For the *ZW*-DOPA/protein G coating, a mixture of *ZW*-DOPA and ammonium persulfate was added to the protein G solution (20 mg/mL) at a 1:1 volume ratio. Then, a substrate was incubated in the *ZW*-DOPA/protein G solution for 2 h at room temperature and washed with PBS buffer containing 0.1% Tween 20 and pure water. Coating of PDA and PDA/protein G was performed through the same procedures using dopamine hydrochloride instead of *ZW*-DOPA.

**Fluorescent Antibody Immobilization.** Each of the surface-modified substrates (bare, PDA, PDA/protein G, *ZW*-DOPA, and *ZW*-DOPA/protein G) was incubated with fluorescent antibody in 0.05% Tween 20 and 1% nonfat milk for 1 h at room temperature. The antibody-immobilized substrates were washed with PBS buffer containing 0.1% Tween 20 and then with pure water three times.

**Protein and *E. coli* Adhesion Test.** GFP solution was prepared at a concentration of 0.5 mg/mL in PBS buffer. Each of the surface-modified substrates was incubated with the GFP solution for 1 h at room temperature. The substrates were gently washed with PBS buffer containing 0.1% Tween 20 and then with pure water. Bare glass, *ZW*-DOPA-coated glass, and *ZW*-DOPA/protein G-coated glass were treated with $10^4$ CFU/mL *E. coli* cultured in LB broth at 37 °C. After incubation at 37 °C for 18 h, the substrates were washed three times and immersed in a dye solution (3 $\mu$M SYTO9 and 3 $\mu$M propidium iodide) at room temperature for 20 min.

**Detection of Influenza Virus with the Naked Eye.** The *ZW*-DOPA/protein G-coated substrates were incubated with the polyclonal anti-influenza A H1N1 antibody (0.1 mg/mL) at room temperature for 1 h and then washed with PBS buffer containing 0.1% Tween 20 and pure water. For the preparation of the immunoprobe, 20 nm Au NPs in PBS (0.1 mM, pH 7.0) were added to GBP-protein G (0.1 mg/mL) and reacted for 16 h at 4 °C. Then, the Au NP-GBP-protein G probe was centrifuged (12 000 rpm, 20 min) at 4 °C and resuspended in 10 mM PBS containing 0.05% Tween 20. The resuspended probe was added to the monoclonal anti-influenza A H1N1 antibody (10 $\mu$g/mL) and reacted at room temperature for 2 h. The Au NP-GBP-protein G-antibody probe was obtained after separation of the unbound antibody by centrifugation (12 000 rpm, 20 min) at 4 °C. For detection of the influenza virus, the prepared pH1N1 solution ($10^7$ PFU/mL) was drop-incubated onto the immune substrates for 1 h at room temperature. Next, the substrates were washed with PBS buffer containing 0.1% Tween 20 and with pure water. The pH1N1-captured substrates were then immersed in the Au NP-GBP-protein G-antibody probe solution at room temperature for 1 h and washed with PBS buffer containing 0.1% Tween 20 and pure water. Finally, Ag enhancer solutions A (silver salt) and B (initiator) were mixed (1:1 v/v) and applied to the substrates. After 5 min, the substrates were washed with pure water and dried with $N_2$ gas.

**Detection of Influenza Virus by SERS.** The *ZW*-DOPA/protein G-coated substrates were incubated with the polyclonal anti-influenza A H1N1 antibody (0.1 mg/mL) at room temperature for 1 h and then washed with PBS buffer containing 0.1% Tween 20 and pure water. For the preparation of the SERS-active immunoprobe, 0.25 mL of $HAuCl_4$ solution (20 mM) was added to 10 mL of HEPES buffer (20 mM, pH 7.4). Next, a solution of MGITC in pure water was added to the urchin Au NP solution with a final MGITC concentration of 20 $\mu$M. This solution was then incubated for 1 h at room temperature. The MGITC-attached urchin Au NPs were added to GBP-protein G (0.1 mg/mL) and reacted for 16 h at 4 °C. Then, the MGITC-urchin Au NP-GBP-protein G probe was centrifuged (12 000 rpm, 20 min) at 4 °C and resuspended in 10 mM PBS containing 0.05% Tween 20. The resuspended urchin Au NPs were added to monoclonal anti-influenza A H1N1 antibody (10 $\mu$g/mL) and reacted at room temperature for 2 h. The MGITC-urchin Au NP-GBP-protein G-antibody probe was obtained after separation of the unbound antibody by centrifugation (12 000 rpm, 20 min) at 4 °C. For the detection of influenza virus, pH1N1 solutions of various concentrations (0, 10, $10^2$, $10^3$, $10^4$, $10^5$, $10^6$, and $10^7$ PFU/mL) were prepared. The prepared pH1N1 solutions were drop-incubated onto the immune substrates at room temperature for 1 h, and the substrates were washed with PBS buffer containing 0.1% Tween 20 and pure water. The pH1N1-captured substrates were then immersed in the SERS-active probe solution for 1 h at room temperature. After washing with PBS buffer containing 0.1% Tween 20 and pure water, the substrates were dried with $N_2$ gas and then SERS spectra were measured. The selectivity test was accomplished through the same procedures using H3N2, H5N2, and IFV B instead of pH1N1.

**Instrumentation.** XPS analyses were performed using a previously reported instrument.[47] Contact angle and thickness measurements were carried out as described previously.[26] AFM images were obtained as described previously.[19] Fluorescence images were measured as described previously.[19] Fluorescence microscope images were obtained using an EVOSFL system (Thermo Fisher Scientific). The binding kinetics of the antibodies on the surface-modified substrates were measured by biolayer interferometry analysis using a BLItz System (ForteBio). Grayscale images and histograms were obtained as described previously.[19] SERS spectra were obtained as described previously.[47]

## ■ ASSOCIATED CONTENT

### Supporting Information

The Supporting Information is available free of charge at https://pubs.acs.org/doi/10.1021/acsabm.0c00264.

Fluorescence images of *E. coli* attached to bare, *ZW*-DOPA-coated, and *ZW*-DOPA/protein G-coated glass substrates (Figure S1); fluorescence images and intensity plots for *ZW*-DOPA/protein G-coated glass substrates after Alexa647-conjugated antibody immobilization (Figure S2); plot of 8-bit grayscale values on *ZW*-DOPA/protein G-coated PET, PS, and PTFE substrates after pH1N1 detection with the naked eye (Figure S3); absorbance spectrum of urchin Au NPs and TEM image of an urchin Au NP (Figure S4); plot of 1615 $cm^{-1}$ band intensity as a function of pH1N1 concentration (Figure S5) (PDF)

## ■ AUTHOR INFORMATION


### Corresponding Authors

**Woo Kyung Cho** − *Department of Chemistry, Chungnam National University, Daejeon 34134, Korea;* orcid.org/0000-0003-1370-4720; Email: wkcho@cnu.ac.kr

**Taejoon Kang** − *Bionanotechnology Research Center, KRIBB, Daejeon 34141, Korea;* orcid.org/0000-0002-5387-6458; Email: kangtaejoon@kribb.re.kr

### Authors

**Jihyun Byun** − *Bionanotechnology Research Center, KRIBB, Daejeon 34141, Korea*

**Soojeong Cho** − *Department of Chemistry, Chungnam National University, Daejeon 34134, Korea*

**Jeong Moon** − *Bionanotechnology Research Center, KRIBB, Daejeon 34141, Korea; Department of Chemical and Biomolecular Engineering, KAIST, Daejeon 34141, Korea*




https://dx.doi.org/10.1021/acsabm.0c00264
ACS Appl. Bio Mater. 2020, 3, 3631−3639

**Hongki Kim** − *Bionanotechnology Research Center, KRIBB, Daejeon 34141, Korea*
**Hyunju Kang** − *Bionanotechnology Research Center, KRIBB, Daejeon 34141, Korea*
**Juyeon Jung** − *Bionanotechnology Research Center, KRIBB, Daejeon 34141, Korea; Department of Nanobiotechnology, KRIBB School of Biotechnology, UST, Daejeon 34113, Korea*
**Eun-Kyung Lim** − *Bionanotechnology Research Center, KRIBB, Daejeon 34141, Korea; Department of Nanobiotechnology, KRIBB School of Biotechnology, UST, Daejeon 34113, Korea;* orcid.org/0000-0003-2793-3700
**Jinyoung Jeong** − *Department of Nanobiotechnology, KRIBB School of Biotechnology, UST, Daejeon 34113, Korea; Environmental Disease Research Center, KRIBB, Daejeon 34141, Korea;* orcid.org/0000-0003-0381-3958
**Hyun Gyu Park** − *Department of Chemical and Biomolecular Engineering, KAIST, Daejeon 34141, Korea;* orcid.org/0000-0001-9978-3890

Complete contact information is available at: https://pubs.acs.org/10.1021/acsabm.0c00264

### Notes

The authors declare no competing financial interest.

## ■ ACKNOWLEDGMENTS

This research was supported by the Basic Science Research Program through the National Research Foundation of Korea (NRF) funded by the Ministry of Science and ICT (MSIT) (NRF-2019R1C1C1006867 and NRF-2019R1A2C4101096), the Center for BioNano HealthGuard funded by the MSIT of Korea as Global Frontier Project (H-GUARD_2013-M3A6B2078950 and H-GUARD_2014M3A6B2060507), the Bio & Medical Technology Development Program of the NRF funded by MSIT of Korea (NRF-2018M3A9E2022821), and the KRIBB Research Initiative Program. J.M. is a recipient of a Global Ph.D. Fellowship (NRF-2019H1A2A1073468).

## ■ REFERENCES

(1) Darwish, I. A. Immunoassay methods and their applications in pharmaceutical analysis: basic methodology and recent advances. *Int. J. Biomed. Sci.* **2006**, *2* (217), 217−235.
(2) Sebba, D.; Lastovich, A. G.; Kuroda, M.; Fallows, E.; Johnson, J.; Ahouidi, A.; Honko, A. N.; Fu, H.; Nielson, R.; Carruthers, E.; et al. A point-of-care diagnostic for differentiating Ebola from endemic febrile diseases. *Sci. Transl. Med.* **2018**, *10*, No. eaat0944.
(3) Hervás, M.; López, M. Á.; Escarpa, A. Electrochemical immunoassay using magnetic beads for the determination of zearalenone in baby food: An anticipated analytical tool for food safety. *Anal. Chim. Acta* **2009**, *653*, 167−172.
(4) Barry, R. C.; Lin, Y.; Wang, J.; Liu, G.; Timchalk, C. A. Nanotechnology-based electrochemical sensors for biomonitoring chemical exposures. *J. Exposure Sci. Environ. Epidemiol.* **2009**, *19*, 1−18.
(5) Yao, S.; Zhao, C.; Liu, Y.; Nie, H.; Xi, G.; Cao, X.; Li, Z.; Pang, B.; Li, J.; Wang, J. Colorimetric Immunoassay for the Detection of Staphylococcus aureus by Using Magnetic Carbon Dots and Sliver Nanoclusters as o-Phenylenediamine-Oxidase Mimetics. *Food Anal. Methods* **2020**, *13*, 833−838.
(6) Wang, Z.; Zong, S.; Wu, L.; Zhu, D.; Cui, Y. SERS-activated platforms for immunoassay: probes, encoding methods, and applications. *Chem. Rev.* **2017**, *117*, 7910−7963.
(7) Trilling, A. K.; Beekwilder, J.; Zuilhof, H. Antibody orientation on biosensor surfaces: a minireview. *Analyst* **2013**, *138*, 1619−1627.
(8) Sharafeldin, M.; McCaffrey, K.; Rusling, J. F. Influence of antibody immobilization strategy on carbon electrode immunoarrays. *Analyst* **2019**, *144*, 5108−5116.
(9) Carpenter, A. C.; Paulsen, I. T.; Williams, T. C. Blueprints for biosensors: design, limitations, and applications. *Genes* **2018**, *9*, No. 375.
(10) Güven, E.; Duus, K.; Lydolph, M. C.; Jørgensen, C. S.; Laursen, I.; Houen, G. Non-specific binding in solid phase immunoassays for autoantibodies correlates with inflammation markers. *J. Immunol. Methods* **2014**, *403*, 26−36.
(11) Ward, G.; Simpson, A.; Boscato, L.; Hickman, P. E. The investigation of interferences in immunoassay. *Clin. Biochem.* **2017**, *50*, 1306−1311.
(12) Tate, J.; Ward, G. Interferences in immunoassay. *Clin. Biochem. Rev.* **2004**, *25*, 105−120.
(13) Lee, H.; Dellatore, S. M.; Miller, W. M.; Messersmith, P. B. Mussel-inspired surface chemistry for multifunctional coatings. *Science* **2007**, *318*, 426−430.
(14) Ryu, J. H.; Messersmith, P. B.; Lee, H. Polydopamine surface chemistry: a decade of discovery. *ACS Appl. Mater. Interfaces* **2018**, *10*, 7523−7540.
(15) Wei, Q.; Yu, B.; Wang, X.; Zhou, F. Stratified polymer brushes from microcontact printing of polydopamine initiator on polymer brush surfaces. *Macromol. Rapid Commun.* **2014**, *35*, 1046−1054.
(16) Chien, H.-W.; Kuo, W.-H.; Wang, M.-J.; Tsai, S.-W.; Tsai, W.-B. Tunable micropatterned substrates based on poly (dopamine) deposition via microcontact printing. *Langmuir* **2012**, *28*, 5775−5782.
(17) Lee, H. A.; Ma, Y.; Zhou, F.; Hong, S.; Lee, H. Material-independent surface chemistry beyond polydopamine coating. *Acc. Chem. Res.* **2019**, *52*, 704−713.
(18) Lynge, M. E.; van der Westen, R.; Postma, A.; Städler, B. Polydopamine—a nature-inspired polymer coating for biomedical science. *Nanoscale* **2011**, *3*, 4916−4928.
(19) Moon, J.; Byun, J.; Kim, H.; Jeong, J.; Lim, E. K.; Jung, J.; Cho, S.; Cho, W. K.; Kang, T. Surface-Independent and Oriented Immobilization of Antibody via One-Step Polydopamine/Protein G Coating: Application to Influenza Virus Immunoassay. *Macromol. Biosci.* **2019**, *19*, No. 1800486.
(20) Kim, S.; Moon, J. M.; Choi, J. S.; Cho, W. K.; Kang, S. M. Mussel-Inspired Approach to Constructing Robust Multilayered Alginate Films for Antibacterial Applications. *Adv. Funct. Mater.* **2016**, *26*, 4099−4105.
(21) Blackman, L. D.; Gunatillake, P. A.; Cass, P.; Locock, K. E. An introduction to zwitterionic polymer behavior and applications in solution and at surfaces. *Chem. Soc. Rev.* **2019**, *48*, 757−770.
(22) Ki, S. H.; Lee, S.; Kim, D.; Song, S. J.; Hong, S.-P.; Cho, S.; Kang, S. M.; Choi, J. S.; Cho, W. K. Antibacterial Film Formation through Iron(III) Complexation and Oxidation-Induced Cross-Linking of *OEG*-DOPA. *Langmuir* **2019**, *35*, 14465−14472.
(23) Sundaram, H. S.; Han, X.; Nowinski, A. K.; Ella-Menye, J.-R.; Wimbish, C.; Marek, P.; Senecal, K.; Jiang, S. One-step dip coating of zwitterionic sulfobetaine polymers on hydrophobic and hydrophilic surfaces. *ACS Appl. Mater. Interfaces* **2014**, *6*, 6664−6671.
(24) Karkhanechi, H.; Takagi, R.; Matsuyama, H. Enhanced antibiofouling of RO membranes via polydopamine coating and polyzwitterion immobilization. *Desalination* **2014**, *337*, 23−30.
(25) Bailey, L. J.; Sheehy, K. M.; Hoey, R. J.; Schaefer, Z. P.; Ura, M.; Kossiakoff, A. A. Applications for an engineered Protein-G variant with a pH controllable affinity to antibody fragments. *J. Immunol. Methods* **2014**, *415*, 24−30.
(26) Yeon, D. K.; Ko, S.; Jeong, S.; Hong, S.-P.; Kang, S. M.; Cho, W. K. Oxidation-Mediated, Zwitterionic Polydopamine Coatings for Marine Antifouling Applications. *Langmuir* **2019**, *35*, 1227−1234.
(27) Hong, D.; Bae, K.; Hong, S.-P.; Park, J. H.; Choi, I. S.; Cho, W. K. Mussel-inspired, perfluorinated polydopamine for self-cleaning coating on various substrates. *Chem. Commun.* **2014**, *50*, 11649−11652.
(28) Kang, S. M.; Hwang, N. S.; Yeom, J.; Park, S. Y.; Messersmith, P. B.; Choi, I. S.; Langer, R.; Anderson, D. G.; Lee, H. One-step

multipurpose surface functionalization by adhesive catecholamine. *Adv. Funct. Mater.* **2012**, *22*, 2949−2955.
(29) Kim, E.-S.; Shim, C.-K.; Lee, J. W.; Park, J. W.; Choi, K. Y. Synergistic effect of orientation and lateral spacing of protein G on an on-chip immunoassay. *Analyst* **2012**, *137*, 2421−2430.
(30) Chen, S.; Li, L.; Zhao, C.; Zheng, J. Surface hydration: Principles and applications toward low-fouling/nonfouling biomaterials. *Polymer* **2010**, *51*, 5283−5293.
(31) Ladd, J.; Zhang, Z.; Chen, S.; Hower, J. C.; Jiang, S. Zwitterionic polymers exhibiting high resistance to nonspecific protein adsorption from human serum and plasma. *Biomacromolecules* **2008**, *9*, 1357−1361.
(32) Ceruso, M. A.; Amadei, A.; Di Nola, A. Mechanics and dynamics of B1 domain of protein G: role of packing and surface hydrophobic residues. *Protein Sci.* **1999**, *8*, 147−160.
(33) Moghadami, M. A narrative review of influenza: a seasonal and pandemic disease. *Iran. J. Med. Sci.* **2017**, *42*, 2−13.
(34) Vemula, S. V.; Zhao, J.; Liu, J.; Wang, X.; Biswas, S.; Hewlett, I. Current approaches for diagnosis of influenza virus infections in humans. *Viruses* **2016**, *8*, No. 96.
(35) Lee, B. W.; Bey, R. F.; Baarsch, M. J.; Simonson, R. R. ELISA method for detection of influenza A infection in swine. *J. Vet. Diagn. Invest.* **1993**, *5*, 510−515.
(36) Ali, T.; Scott, N.; Kallas, W.; Halliwell, M. E.; Savino, C.; Rosenberg, E.; Ferraro, M.; Hohmann, E. Detection of influenza antigen with rapid antibody-based tests after intranasal influenza vaccination (FluMist). *Clin. Infect. Dis.* **2004**, *38*, 760−762.
(37) Dziąbowska, K.; Czaczyk, E.; Nidzworski, D. Detection methods of human and animal influenza virus—current trends. *Biosensors* **2018**, *8*, No. 94.
(38) Howes, P. D.; Chandrawati, R.; Stevens, M. M. Colloidal nanoparticles as advanced biological sensors. *Science* **2014**, *346*, No. 1247390.
(39) Batul, R.; Tamanna, T.; Khaliq, A.; Yu, A. Recent progress in the biomedical applications of polydopamine nanostructures. *Biomater. Sci.* **2017**, *5*, 1204−1229.
(40) Schlücker, S. Surface-Enhanced raman spectroscopy: Concepts and chemical applications. *Angew. Chem., Int. Ed.* **2014**, *53*, 4756−4795.
(41) Tang, H.; Zhu, C.; Meng, G.; Wu, N. Surface-enhanced Raman scattering sensors for food safety and environmental monitoring. *J. Electrochem. Soc.* **2018**, *165*, B3098−B3118.
(42) Qian, X.; Peng, X.-H.; Ansari, D. O.; Yin-Goen, Q.; Chen, G. Z.; Shin, D. M.; Yang, L.; Young, A. N.; Wang, M. D.; Nie, S. In vivo tumor targeting and spectroscopic detection with surface-enhanced Raman nanoparticle tags. *Nat. Biotechnol.* **2008**, *26*, 83−90.
(43) Leng, W.; Vikesland, P. J. MGITC facilitated formation of AuNP multimers. *Langmuir* **2014**, *30*, 8342−8349.
(44) Bakr, O. M.; Wunsch, B. H.; Stellacci, F. High-yield synthesis of multi-branched urchin-like gold nanoparticles. *Chem. Mater.* **2006**, *18*, 3297−3301.
(45) Eom, G.; Hwang, A.; Lee, D. K.; Guk, K.; Moon, J.; Jeong, J.; Jung, J.; Kim, B.; Lim, E.-K.; Kang, T. Superb Specific, Ultrasensitive, and Rapid Identification of the Oseltamivir-Resistant H1N1 Virus: Naked-Eye and SERS Dual-Mode Assay Using Functional Gold Nanoparticles. *ACS Appl. Bio Mater.* **2019**, *2*, 1233−1240.
(46) Lee, K. J.; Lee, W. S.; Hwang, A.; Moon, J.; Kang, T.; Park, K.; Jeong, J. Simple and rapid detection of bacteria using a nuclease-responsive DNA probe. *Analyst* **2017**, *143*, 332−338.
(47) Kim, H.; Jang, H.; Moon, J.; Byun, J.; Jeong, J.; Jung, J.; Lim, E.-K.; Kang, T. Metal−Organic Framework Coating for the Preservation of Silver Nanowire Surface-Enhanced Raman Scattering Platform. *Adv. Mater. Interfaces* **2019**, *6*, No. 1900427.


https://dx.doi.org/10.1021/acsabm.0c00264
*ACS Appl. Bio Mater.* 2020, 3, 3631−3639